Supporting Information

Emulating Frog's behavior: Humidity-Driven Paired-Pulse Facilitation and Metaplasticity realised in a 1D Supramolecular Nanofibre based neuromorphic device

Sukanya Baruah[1,†], Tejaswini S. Rao[1,†], Subi J. George[2], Giridhar U. Kulkarni[1,*]

[1]Chemistry & Physics of Materials Unit, Jawaharlal Nehru Centre for Advanced Scientific Research, Jakkur P. O., Bangalore-560064, India.

[2]Supramolecular Chemistry Laboratory, New Chemistry Unit, Jawaharlal Nehru Centre for Advanced Scientific Research, Jakkur P. O., Bangalore-560064, India.

†Sukanya Baruah and Tejaswini S. Rao contributed equally to this work.

Email- kulkarni@jncasr.ac.in

Device geometry	Lateral or Vertical (L/V)	Organic or Inorganic (O/I)	Dimensionality (0/1/2/3D)	Stimuli Electrical-E Optical-O Humidity-H Pressure-P	Tunability of PPF	Multi stimuli operation	Metaplasticity	Ref
graphene/hBN/CsPbBr3 QDs	L	I	0D-2D heterostructure	O, E	×	×	×	1
Au/Gelatin-PEDOT:PSS/Al	V	O	2D	E, H	×	✓	×	2
Ag/$CsPbBr_3$/PVA/FTO	V	I	2D	E, P	×	×	×	3
Au/CuPc/Au	L	O	2D	O, E	×	×	×	4
Au/ZnO/Au	L	I	2D	O	×	×	×	5
Au/P3HT/ITO	V	O	2D	O	×	×	×	6
ITO/$(R/S\text{-}MBA)_2PbI_4$/PMMA/Al	V	Hybrid	2D	O, E	✓	×	×	7
Ag/$CdPS_3$/ITO	V	I	2D	E	×	×	×	8
Au/C8-BTBT: P3HT/Au	L	O	2D	O, E	×	×	×	9
This work	L	O	1D	O, H	✓	✓	✓	

Table S1- Comparison of two terminal neuromorphic devices and their potential to exhibit tunable PPF, multi stimuli operation, and metaplasticity

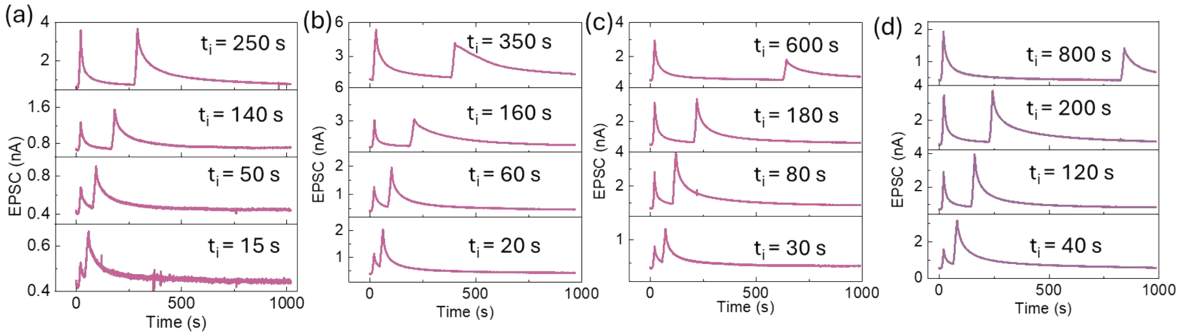

Figure S1. (a)-(d) Response of the nanofibres with two 75% RH pulses (t_w = 15 s) where t_i was varied from 15 s to 800 s and monitored at 40% RH.

Figure S1 shows the remaining representative response curves for different t_i, utilised for PPF calculation in Figure 2c. Considering t_i = 20 s (Figure S1b), current increases from 0.4 nA (A_0) to 1.1 nA with the application of the first RH pulse (75%) and finally increases to 2 nA with the second RH pulse, showing facilitation with a PPF index of 2.2.

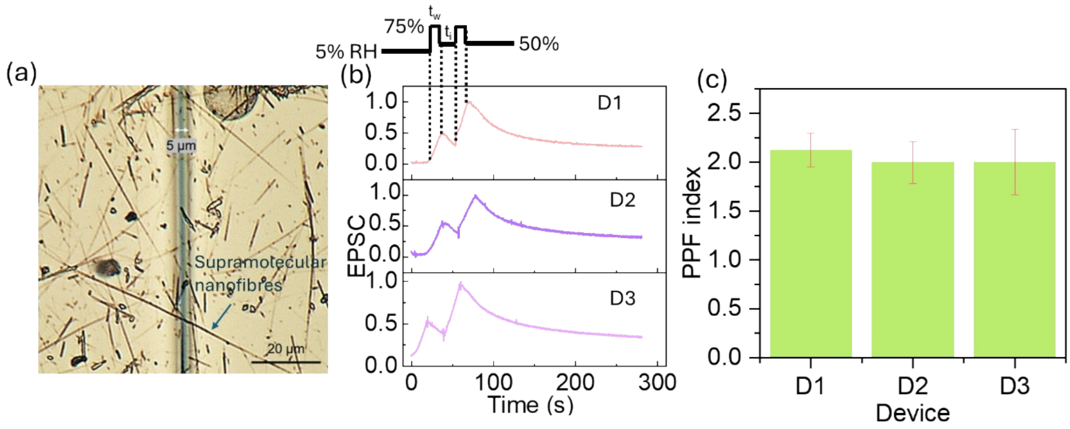

Figure S2. Device-to-device variability. (a) Optical image of the nanofibre device with nanofibres spread across a 5 µm gap Ti electrodes. (b) Response to two 75% RH pulses with $t_w = t_i$ = 15 s for 3 different devices. (c) Average PPF index achieved for 3 devices, with error bars standing for 5 measurements each.

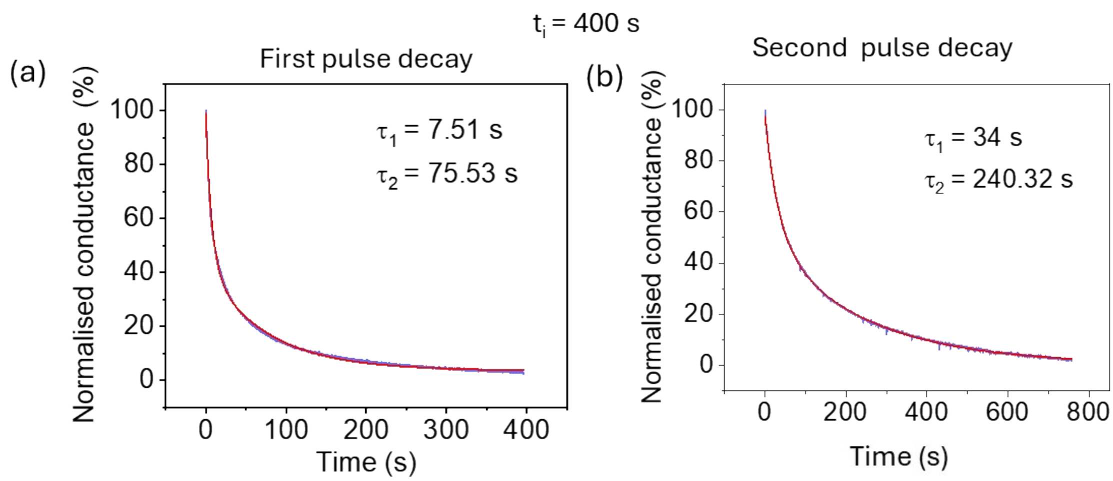

Figure S3. (a-b) Double exponentially fitted decay curves post first pulse and second pulse, considering percentage decay till 3% of maximum EPSC with τ_1 and τ_2 mentioned in the inset.

The decay post first and second pulse has been fitted with a double exponential function. The percentage of decay during t_i (after the first pulse) is considered, and the same decay percentage has been utilized during the second pulse decay fitting. This has been done at all the t_i's.

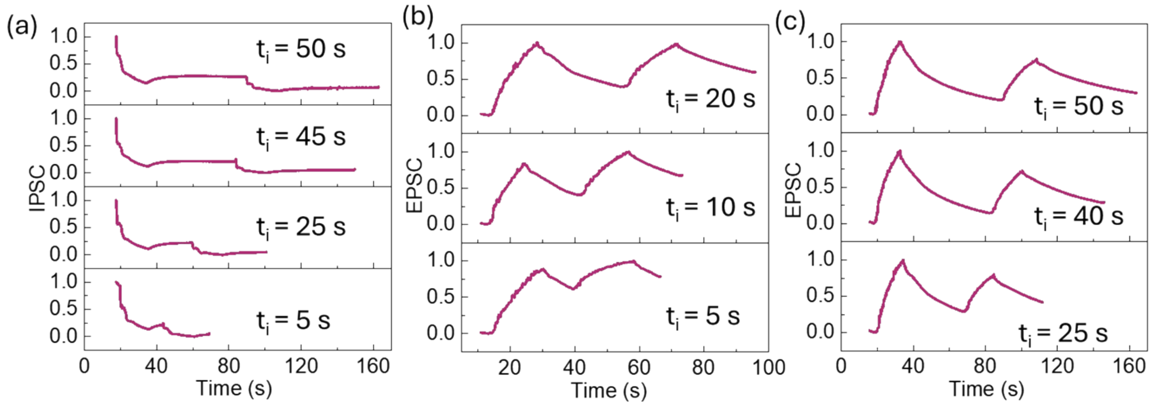

Figure S4. (a) Response curves for different t_i for showing PPD with 5% RH pulses (t_w = 15 s) with other parameters as described in Figure 3a. (b-c) Response curves for different t_i for showing PPF with 75% RH pulses (t_w = 15 s) as described in Figure 3c, and t_i is monitored at 40% RH.

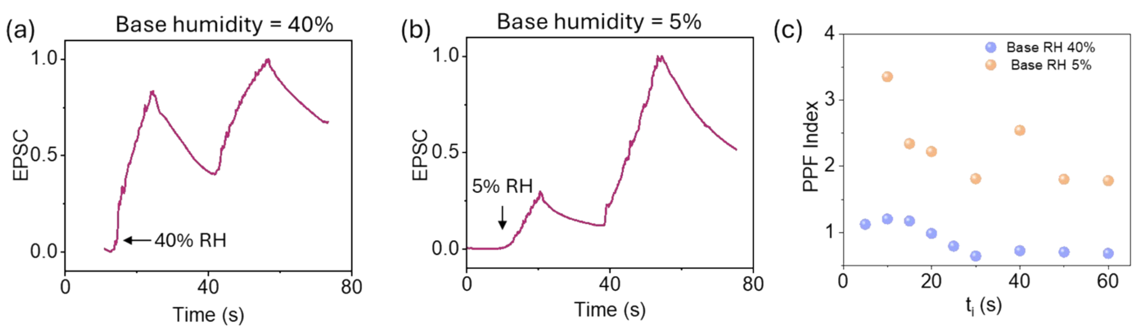

Figure S5. Comparison of base humidity-dependent facilitation in the device with base (a) 40% RH, (b) 5% RH, t_w = 15 s, t_i = 15 s (c) Variation in PPF index with two different base RH.

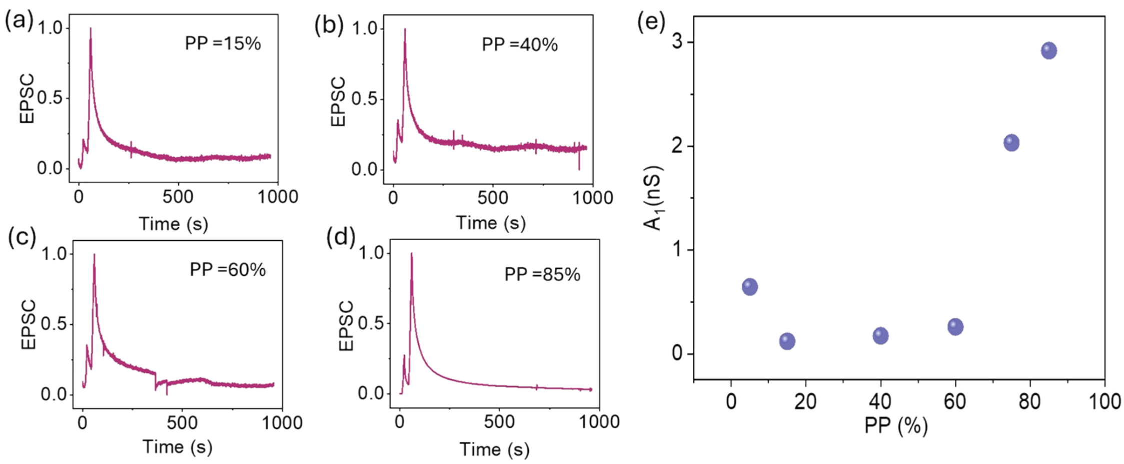

Figure S6. Priming protocol discussed in Figure 4d. Priming pulse RH was varied from (a) 15% to (d) 85% with PP of 5 minutes, and post-PP delay is 5 minutes, and responses were recorded with 75% RH (TP) with t_w=t_i= 15 s and t_i monitored at 40% RH. (e) A_1 plotted with increasing PP.

The remaining response curves (Figure S6a–d) corresponding to the PPF index in Figure 4d indicate a similar A_2/A_1 ratio across all priming conditions. A_1 maintains a similar value till 60% PP RH proves that 5 minutes of post-PP delay is sufficient to diminish the effect of Priming (Figure S6e).

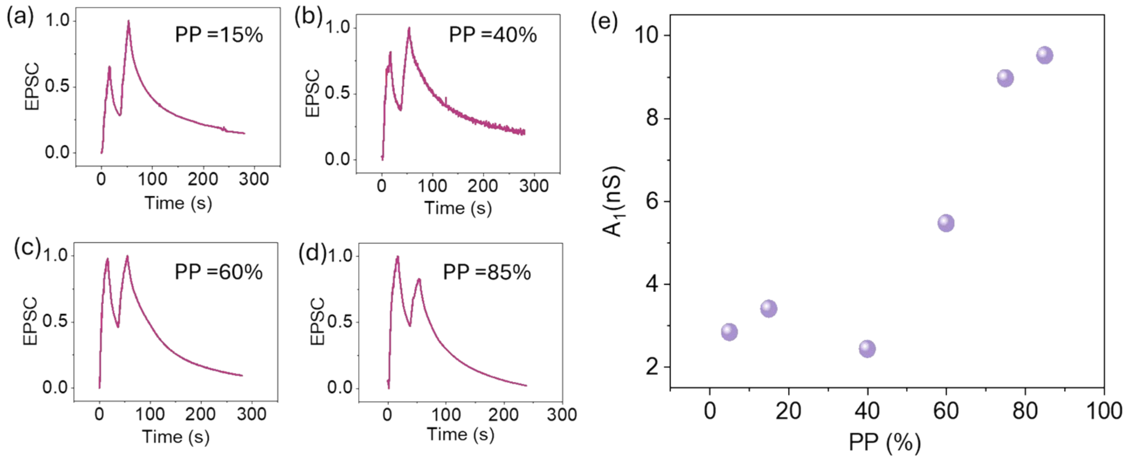

Figure S7. Priming protocol discussed in Figure 4g. Priming pulse RH was varied from (a) 15% to (d) 85% with t_w of 2 minutes, and post PP delay is 20 s, and responses were recorded with 75% RH (TP) with t_w=t_i= 15 s and t_i monitored at 40% RH. (e) A_1 variation with varying PP.

The remaining representative response curves for the index shown in Figure 4g explain that with increasing PP, A_2 decreases with respect to A_1 (Figure S7a-d). A_1 shows an increasing trend with increasing PP (Figure S7e), proving the influence of PP, with 20 s post-PP delay on the nanofibres.

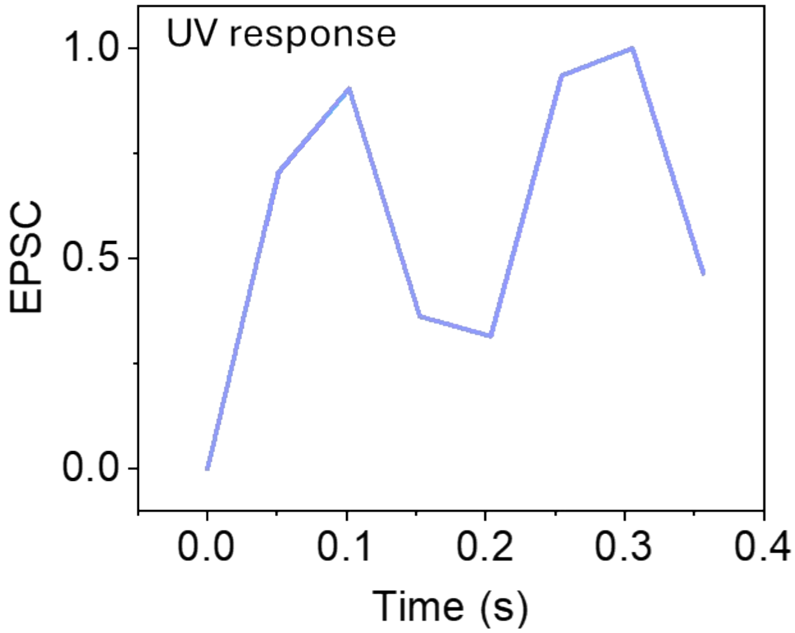

Figure S8. Response with UV light of wavelength 365 nm ($t_i = t_w = 100$ ms) and power 20.5 mW.

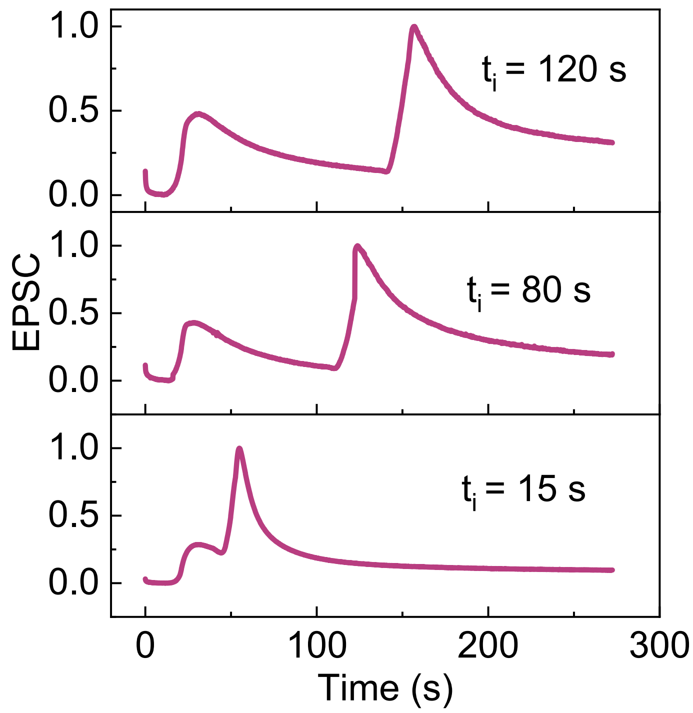

Figure S9. Remaining response curves for PPF index shown in Figure 5c (with light), where 75% RH pulses with t_w of 10 s were applied with continuous light illumination. t_i was varied from 15 to 120 s, monitored at 40% RH.

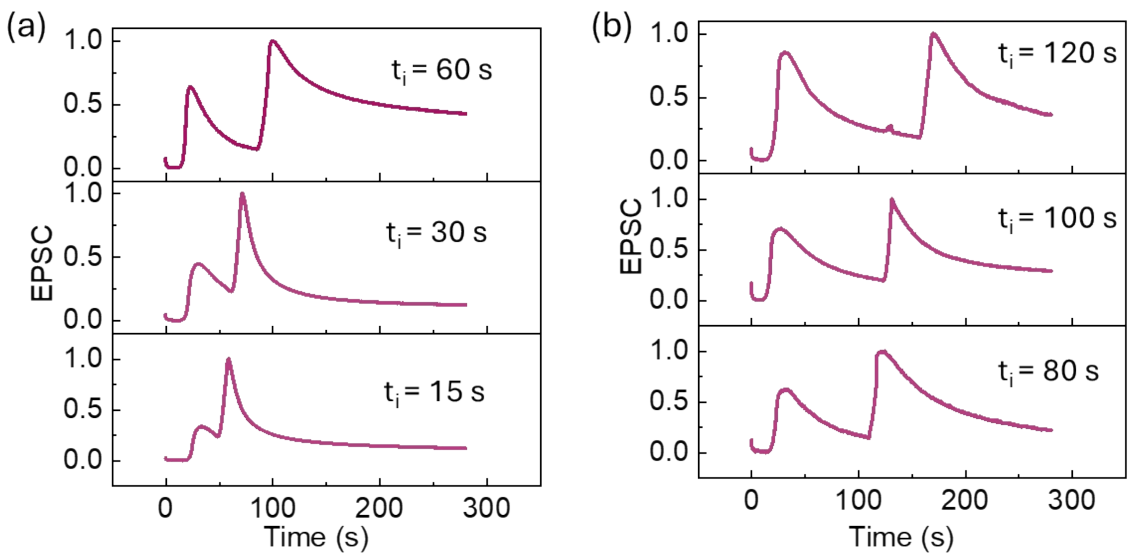

Figure S10. Response curves for the PPF index, shown in Figure 5c, without light show a lower PPF index as compared to that with light.

References

1 C. Han, X. Han, J. Han, M. He, S. Peng, C. Zhang, X. Liu, J. Gou and J. Wang, *Adv Funct Mater*, 2022, 32, 2113053.

2 R. Sadhukhan, S. P. Verma, S. Mondal, A. Das, R. Banerjee, A. Mandal, M. Banerjee and D. K. Goswami, *Small*, 2024, 20, 2307439.

3 D. Chen, X. Zhi, Y. Xia, S. Li, B. Xi, C. Zhao and X. Wang, *Small*, 2023, 19, 2301196.

4 A. B. Mishra and R. Thamankar, *Nanoscale*, 2024, 16, 18597–18608.

5 W. Xiao, L. Shan, H. Zhang, Y. Fu, Y. Zhao, D. Yang, C. Jiao, G. Sun, Q. Wang and D. He, *Nanoscale*, 2021, 13, 2502–2510.

6 P. Zhao, R. Ji, J. Lao, W. Xu, C. Jiang, C. Luo, H. Lin, H. Peng and C.-G. Duan, *Org Electron*, 2022, 100, 106390.

7 S. Dan, S. Paramanik and A. J. Pal, *ACS Nano*, 2024, 18, 14457–14468.

8 Z. Peng, Z. Cheng, S. Ke, Y. Xiao, Z. Ye, Z. Wang, T. Shi, C. Ye, X. Wen, P. K. Chu, X.-F. Yu and J. Wang, *Adv Funct Mater*, 2023, 33, 2211269.

9 Y. Ni, L. Yang, J. Feng, J. Liu, L. Sun and W. Xu, *SmartMat*, 2023, 4, e1154.